BEST: International Journal of Management, Information Technology and Engineering (BEST: IJMITE)
ISSN (P): 2348-0513, ISSN (E): 2454-471X,
Vol. 4, Issue 12, Dec 2016, 1-22

DESIGN AND SIMULATION OF AN EXHAUST BASED THERMOELECTRIC GENERATOR (TEG) FOR WASTE HEAT RECOVERY IN PASSENGER VEHICLE

GOVINDU ECHARLA[1] & SUDHAKAR UPPALAPATI[2]

[1]M.Tech (Cad/Cam) Final Year Marri Laxman Reddy Institute of Technology &Management, Hyderabad, India

[2]Assistant Professor Marri Laxman Reddy Institute of Technology &Management, Hyderabad, India

ABSTRACT

The increasing demand for electric power in passenger vehicles has motivated several research focuses since the last two decades. This demand has been revolted by the unrelenting, rapidly growing reliance on electronics in modern vehicles. Generally, internal combustion engines lose more than 35% of the fuel energy in exhaust gas. Comparing this huge loss to every day's growing oil price, one could understand how the recovery of such losses could help the economy, as well as providing the additional power sources required by contemporary vehicle systems. There are three fundamental advantages of thermoelectric generators (TEGs) over other power sources; they do not have any moving parts as they generate power using Seebeck solid-state phenomena, they have a long operation lifetime, and they can be easily integrated to any vehicle's exhaust system. This project presents a novel TEG concept aims to resolve the thermal and mechanical disputes faced by the research community. Several simulation models are used to analyse the TEG performance. The significance of the novel TEG is discussed through a detailed comparison with experimental results from Clarkson University TEG prototype tests. The simulation results showed a huge increase in the power generated.

KEYWORDS: Thermoelectric Generators, Seebeck Solid-State Phenomena

INTRODUCTION

The expression "Energy Crisis" has become a symbol of the human concern about the increasing demands and consumption of energy on earth. For almost two hundred years, the main energy resource has been fossil fuel. The world consumption of all energy resources is forecasted to increase from 421 quadrillion Btu in 2003 to 563 quadrillion Btu in 2015 then to 722 quadrillion Btu in 2030, as shown in Figure 1.1.

Figure 1.1: World Market Energy Consumption 1980 – 2030, (IEO, 2006)

Fossil fuels continue to supply much of the increment in marketed energy use worldwide throughout the next two and half decades. Oil remains the dominant energy source, but its share of total world energy consumption declines from

38 % in 2003 to 33 % in 2030 as illustrated in Figure 1.2, largely in response to higher world oil prices, which will dampen oil demand in the mid-term. Worldwide oil consumption is expected to rise from 80 million barrels per day in 2003 to 98 million barrels per day in 2015 and then to 118 million barrels per day in 2030.

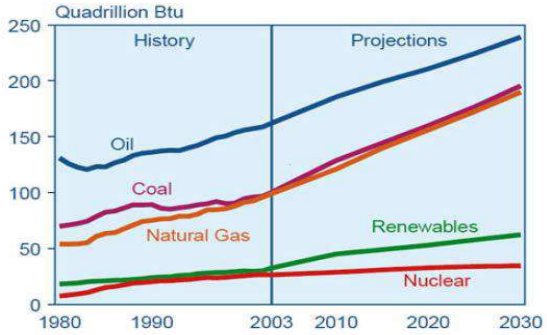

Figure 1.2: World Market Energy Use by Fuel Type 1980 – 2030, (IEO, 2006)

Trends of Energy Usage in Road Transport Sector

The transport sector will account for 54% of global primary oil consumption in 2030 compared to 47% now and 33% in 1971, as demonstrated in Figure 1.3. Transport will absorb two-thirds of the increase in total oil use. Almost all the energy currently used for transport purposes is in the form of oil products. Share of oil in transport energy demand will remain almost constant over the projection period, at 95%, despite the policies and measures that many countries have adopted to promote the use of alternative fuels such as biofuels and compressed natural gas. (WEO, 2004)

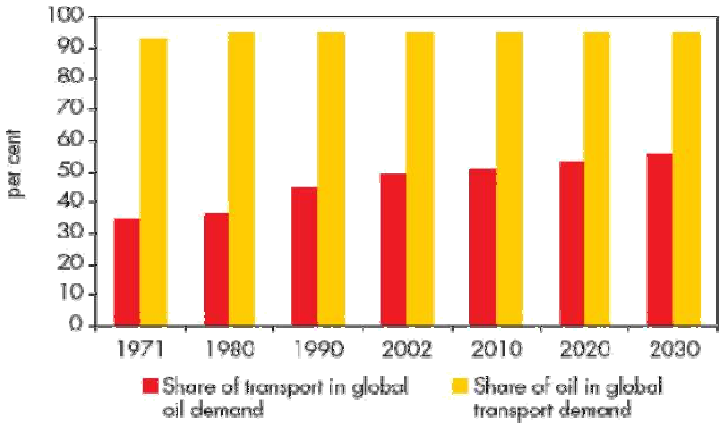

Figure 1.3: Reciprocal Transport and Oil Demands

The demand for road transport fuels is growing dramatically in many developing countries, in line with rising incomes and infrastructure development. The passenger car fleet in China – the world's fastest growing new-car market – grew by more than 9% per year in the five years to 2002, compared to just over 3% in the world as a whole as reported by Rueil and Malmaison (2003). Preliminary data show that more than two million new cars were sold in China in 2003. The scope for continued expansion of the country's fleet is enormous: there are only 10 cars for every thousand Chinese people compared with 770 in North America and 500 in Europe. Other Asian countries, including Indonesia and India, are also experiencing a rapid expansion of their car fleets. Freight will also contribute to the increase in oil use for transport in all regions. Most of the increased freight will travel by road, in line with past trends.

Thermoelectric Waste Heat Recovery as a Potential Energy Efficiency Option in Ground Vehicles

Stabler (2002) reported that in gasoline powered internal combustion engines; roughly 40% of the fuel energy is wasted in exhaust gases, and 30% in engine coolant. On the other hand, in diesel powered internal combustion engines about 25% and 35% of the fuel energy are wasted in the engine exhaust and coolant systems respectively. Unfortunately, present-day engine designs may not meet all our future needs. In order to meet the rapidly increasing requirements of electrical power the OEMs are considering several alternatives like 42 volt systems, hybrid vehicles, fuel cell vehicles, and so on. One such alternative is the use of thermoelectric generators to recover the waste heat from the exhaust and/or the engine coolant.

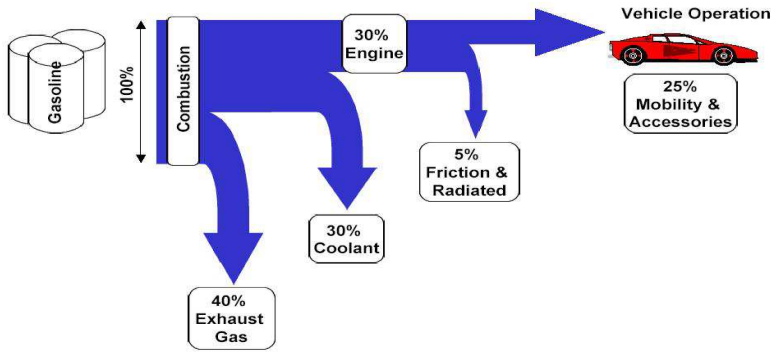

Figure 1.4: Energy Path in Gasoline Fueled Internal Combustion Engine Vehicle

Thermoelectric generators utilize the Seebeck thermoelectric effect to generate electric current from a temperature gradient. The discovery of Seebeck effect dates back to 1821, however, the interest in utilizing this physical phenomenon in automobiles started only in the second half of the twentieth century.

Thermoelectric generators are expected to achieve up to 10% fuel economy through offering more electric power for automobile systems. Within 8 to 12 years, thermoelectric generator would be able to save up to 10% and 16% in light and heavy duty trucks respectively. While hydrogen fuel cells still face obstacles in the design and implementation of their refuelling facilities, thermoelectric generators, unbelievably, are predicted to be the potential alternatives of internal combustion engines after 25 years (Fairbanks 2005).

A thermoelectric generator with an efficiency of 20% would allow for a reduction in fuel consumption incrementing the useful power from a gasoline ICE to a maximum of 52% (Kushch et al. 2001). In order to achieve such efficiency from the current state-of-the art thermoelectric generators which have an efficiency of 5~8%; several challenges should be encountered. The thermoelectric generator efficiency is directly dependant on the conversion efficiency of the materials employed and the overall efficiency of the heat exchangers. Saqr*et al.* (2007) stated that while there is a rat race to produce more efficient, less expensive, and more durable thermoelectric materials, the research community is reluctantly interested in improving the thermoelectric generators' heat exchanger systems in terms of thermal and mechanical efficiencies. For the exhaust-based thermoelectric generators, the overall efficiency of the system is the product of three terms; two of them represent the thermal effectiveness of the generator heat exchangers, while the third is the thermoelectric conversion efficiency of the materials employed (Ikoma et al. 1998). There are several options to investigate in order to enhance the thermal efficiency of thermoelectric generators; including the use of highly conducting alloys, innovative heat enhancement techniques in both cold and hot side heat exchangers, and reducing the overall weight

through creative and innovative assembly.

Research Objectives

The main objective of this research is to conceptualize and design an exhaust based thermoelectric generator that overcomes the thermal shortcomings found in earlier models of thermoelectric generators. The design process includes a performance simulation for the thermoelectric generator. Secondary objectives for this research are:

- Establish a novel procedure for design of thermoelectric generators
- Explore the potential of thermoelectric generators as a source of electric power onboard automobiles through the previous, current and future research and commercial trends worldwide.

Simulation Strategy

Working fluids in thermoelectric generators for automobile waste heat recovery are the exhaust gases and the engine cooling water for the hot and cold sides respectively. Exhaust gases temperature varies with engine speed and volumetric efficiency. While cooling water temperature varies mostly between 50 $^{\circ}$c to 80 $^{\circ}$c for light duty vehicles during engine part load. The performance of optimized heat exchanger is simulated using ANSYS FLUENT in order to predict the performance characteristics.

FUNDAMENTALS OF THERMOELECTRIC POWER GENERATION

Seebeck Effect

The principle behind thermoelectric power generation is “SEEBECK EFFECT”. In 1821, Seebeck reported his results to the Prussian Academy of Sciences, which endorsed that he had observed the first of the thermoelectric effects to be discovered. He had produced potential differences by heating the junctions between dissimilar conductors. Despite of the fact that he did not fully understand the meaning of his results, Seebeck was able to arrange his conductors in more or less to the thermoelectric series which is known today. According to Seebeck Effect, a voltage is produced in a closed circuit of two dissimilar metals if the two junctions are maintained at different temperatures, as in thermocouples (fig 2.1).An open circuit potential difference (V) is developed as a result of the temperature difference (T) between the junctions of conductor a to conductor b. The differential Seebeck coefficient,

$$\alpha = \Delta V / T \qquad (2.1)$$

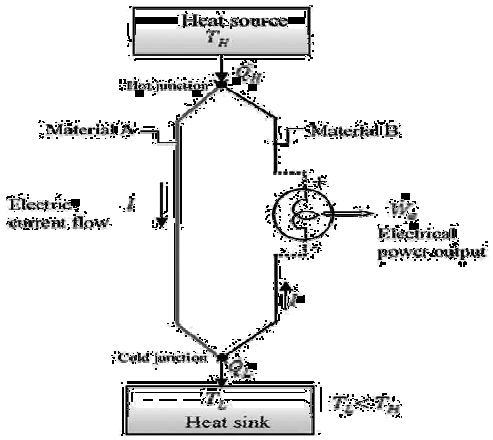

Figure 2.1: Principle of Seebeck Effect

Semiconductors in Teg

Thermoelectric power generation (TEG) devices typically use special semiconductor materials, which are optimized for the Seebeck effect. A thermoelectric pair, composed of a P-type and N-type semiconductors is used. These pairs are connected electrically in series and thermally in parallel in power generation mode to form a module.

Thermoelectric Molecular Explanation

A molecular model is necessary to explain the thermoelectric phenomena. Most elements in the periodic table exist as metals and exhibit electrical and magnetic properties unique to each of them. Furthermore, it is a common knowledge that the properties of alloys are different from those of their constituent elemental metals. Likewise, semiconductors and insulators consisting of a combination of several elements can also be formed. A molar quantity of a solid contains as many as 10^{23} atoms (Mizutani, 2001). A solid-phase of any material is created as a result of bonding among such a huge number of atoms. The entities responsible for the bonding are the electrons. The physical and chemical properties of any solid are results of how the constituent atoms are bonded together through the interaction of their electrons among themselves and with the potentials of the ions. Electricity is the movement of electrons in a circuit. Conductivity takes a somewhat different form when it comes to semiconductor material. For thermoelectric applications, semiconductor materials are 'grown' into crystalline structures which are given conductive properties by virtue of the impurities (i.e. dopants) which are added. In their purest form (i.e., without dopants), the base semiconductor materials form crystalline lattices which become very stable by sharing electrons among the constituent atoms.

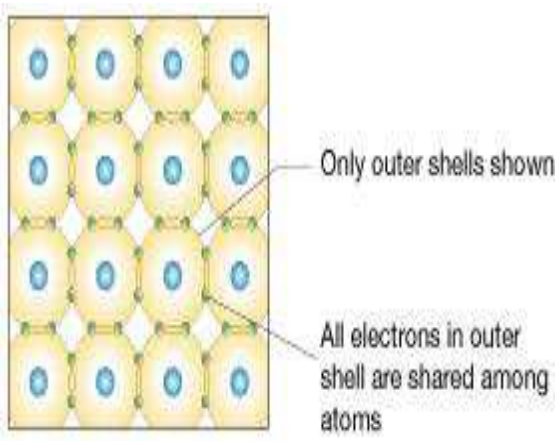

Figure 2.2: Atomic Configuration of a Silicon Crystal

Figure 2.2 shows such a configuration for a silicon crystal. In looking at the shell mapping, it is noticed that the electrons (shown in green), are actually in constant motion as they orbit the nuclei in the lattice. The shared electrons, however, are continually pulled into the orbits of adjacent nuclei to maintain the structural stability of the lattice. In this pure state, the material is not very conductive. Once the impurities are added to the mix, however, the conductive properties are radically affected. For example, if a crystal is formed primarily of silicon (which has four valence electrons), and arsenic impurities (having five valence electrons) are added, there will be free electrons which do not fit into the crystalline structure, as shown in Figure 2.3.

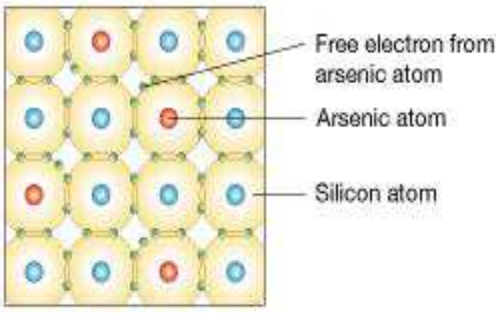

Figure 2.3: Crystalline Structure of Negative Doped (N-Type) Silicon-Arsine Thermoelectric Material

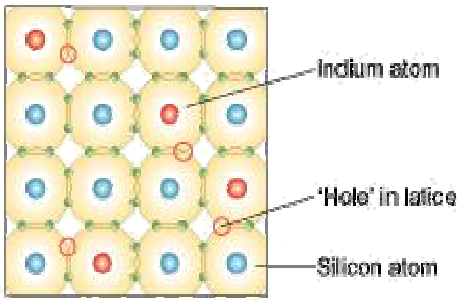

Figure 2.4: Crystalline Structure of Positive Doped (P-Type) Silicon-Indium Thermoelectric Material

These electrons are thus 'loosely bound' and when a voltage is applied, they can be easily set in motion to allow electrical current to pass. The loosely bound electrons are considered the charge carriers in this 'negatively doped' material (which is referred to as 'N' material). It is also possible to form a more conductive crystal by adding impurities which have one less valence electron. For example, if Indium impurities (which have three valence electrons) are used in combination with silicon, this creates a crystalline structure which has 'holes' in it—that is, places within the crystal where an electron would normally be found if the material was pure (see Figure 2.4).

These 'holes' make it much easier to convey electrons through the material upon the application of a voltage. In this case, 'holes' are considered to be the charge carriers in this 'positively doped' conductor v(which is referred to as 'P' material). It is critical here to understand that the existence of charge carriers is exclusively a material dependant property. The immense majority of conductors employs electrons as the charge carriers and considered as 'N' material.

It is through the use of both N and P type materials in a single power generation device, that we can truly optimize the Seebeck effect. As shown in Figure 2.5, the N and P pellets are configured thermally in parallel, but electrically in a series circuit. Because electrical current (i.e., moving electrons) flows in a direction opposite to that of positive charge carriers (i.e. holes) flow, the current generating potentials in the pellets do not oppose one another, but are series-aiding. Thus, if each pellet developed a Seebeck voltage of 20 mV, this combination of an N and P pellet would generate approximately 40 mV rather than zero volts. The voltage output from semiconductor thermocouples remains relatively low; hundreds of micro volts per degree, and in practice a large number of thermocouples are connected electrically in series and thermally in parallel by Sandwiching them between two high thermal conductivity but low electrical conductivity ceramic plates to form a module (see Figure 2.6).

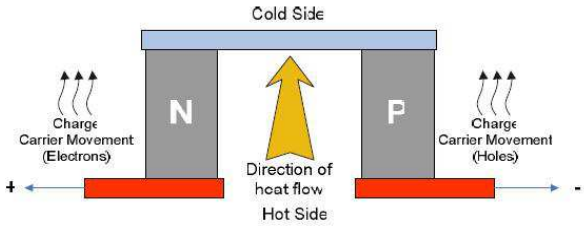

Figure 2.5: A Thermoelectric Pair

The module is the building-block of a thermoelectric conversion system. Ideally, the geometry of the thermo elements should be wire-like (long and thin) for power generation and squat (short and fat) for refrigeration (Rowe, 2005).

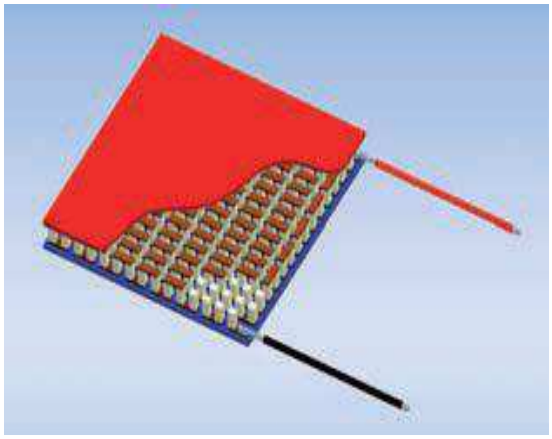

Figure 2.6: Schematic of a Thermoelectric Module Showing the P and N Thermoelectric Pairs

Thermoelectric Generator Efficiency

A thermoelectric generator is a heat engine, and like all heat engines, it obeys the laws of thermodynamics. If we first consider the converter operating as an ideal generator in which there are no heat losses, the efficiency is defined as the ratio of the electrical power delivered to the load to the heat supplied at the hot junction. Consider the simplest generator consisting of a single thermocouple with thermo elements fabricated from N-type and P-type semiconductors. The efficiency of the generator is given by:

$$\eta = \frac{\text{Electrical energy supplied to the load}}{\text{Heat energy absorbed at hot junction}} \quad (2.2)$$

General Concept of Thermoelectric Waste Heat Recovery in Automobiles

In automobiles, waste heat can be recovered from the exhaust gas and/or engine coolant. In exhaust waste heat recovery, thermoelectric conversion modules are stacked between two different heat exchangers. The hot-side heat exchanger is designed to extract heat from the exhaust gas, while the cold-side heat exchanger is designed to dissipate this heat after passing through the thermoelectric modules. On the other hand, in coolant waste heat recovery, the hot side heat exchanger is designed to extract heat from the engine coolant. The cold-side heat exchanger may dissipate heat either to the engine coolant in case of exhaust waste heat recovery, or to the ambient air in the coolant waste heat recovery. The heat cannot be dissipated to the ambient in case of exhaust waste heat recovery because this type of heat exchangers usually

requires some sort of turbulence around its fins to achieve high overall heat transfer coefficient. The absence of this turbulence in cases of engine idling and at the beginning of parking mode puts the thermoelectric modules into an overheating risk because of the high temperature of the exhaust gases.

Figure 2.6 Schematic of a thermoelectric module showing the P and N thermoelectric pairs.

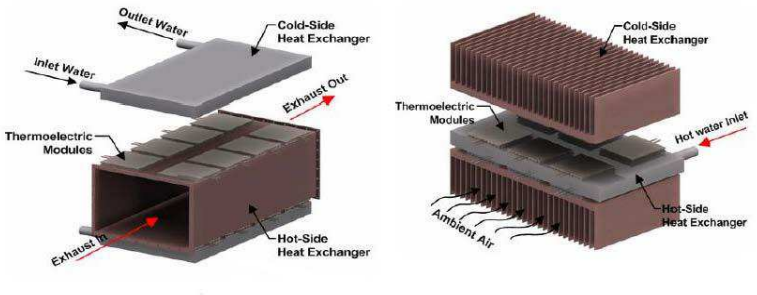

(A) (B)

Figure 2.7: (A) Exhaust Based Waste Heat Recovery TEG; (B) Coolant Based Waste Heat Recovery TEG

In diesel engines 16% ~ 35% of the fuel energy is rejected in engine coolant (i.e. water) compared to 17%~26% in gasoline engines. For this reason coolant based waste heat recovery is more favoured for diesel than gasoline engines. Conversely, exhaust waste heat recovery is more favoured for gasoline than diesel engine for the reason that 34%~45% of the gasoline fuel energy is wasted in exhaust compared to 22%~ 35% of the diesel fuel energy wasted in diesel engine. The main key terms argued when developing exhaust based TEG are the heat exchanger(s) effectiveness, thermoelectric modules efficiency and TEG own weight. In order to increase the hot-side heat exchanger effectiveness, a certain level of turbulence should be achieved with the exhaust flow to increase the overall heat transfer coefficient of the gas. While for the cold-side heat exchanger, the added cooling load should be taken into account to retrofit the engine coolant circuit to determine the optimum coolant flow rate into the heat exchanger. The conversion efficiency of the thermoelectric modules is a direct function in temperature difference across the module thickness. The conversion efficiency at a maximum power output is given by the following equation,TEG technology shall be able to offer 10% fuel economy within 3 to 5 years time. Within 8 to 12 years time, they predict that the fuel economy gains should reach 20%. After 25 years, the internal combustion engine is forecasted to be replaced totally by thermoelectric generators driven combustion champers that can burn any type of fuel (Fairbanks, 2005). This advance in the efficiency of thermoelectric materials and system is expected to be joined with a reduction in the cost per unit energy produced by thermoelectrics.

LITERATURE REVIEW

Thermoelectric generators along their history have covered a huge area of applications, starting from domestic to aerospace. This chapter draws a timeline for the evolution of thermoelectric generators with their different applications and capacities, and focuses intensively on thermoelectric vehicular waste heat recovery generators.

Thermoelectric Materials

Presently, thermoelectric materials for power generation purposes are based on PbTe at low and moderate

temperature gradient applications. In higher temperature gradients, SiGe alloys are employed. FeSi is used for high temperature applications as well. Additionally, iron silicates have a very strong durability at high temperatures and mechanical stresses. The advances in thermoelectric Figure of merit during the last 60 years were astonishing, taking the Z value from 0.5 in late 1950s to 3.5~4 in 2007.

The implementation of Quantum-well technology in thermoelectric materials promises to increase the efficiency of thermoelectric as energy conversion alternatives to reach 35% by the year 2030.

Thermoelectric Generator Applications in Vehicles

The first thermoelectric generator for exhaust heat recovery in vehicles was introduced in 1963 (Neild, 1963). In fact, the potential of thermoelectric as energy-efficiency systems in automobiles has increased dramatically with the discovery of more effective and cheaper materials. However, the mentioned system has not been introduced commercially until this very moment, although several researches are driven to achieve this objective in the near future.

Clarkson University TEG – USA

The experimental results of a 300 W ETEG were reported in 2004 by Kushch et al. The project team joined Clarkson University and Delphi Systems and was funded by NYSERDA and DOE to develop a 300 W ETEG to be mounted on a GM sierra pickup truck (Kushsch et al, 2004). In order to achieve the power goal, a total number of 16 HZ 20 thermoelectric modules were used. Eight modules were mounted on each side of the carbon steel hot box, and all the modules were connected electrically in series and thermally in parallel. The HZ-20 bismuth telluride based modules generates 19 W at minimum if the temperature difference between the two sides of the modules is 200ºC.The module dimensions are 75 × 75× 5 mm, and the weight is115 gm. The TEMs were assembled at a preload pressure of 200 psibetween the hot box and two aluminium water jackets. The overall dimensions of the ETEG were 330 × 273 × 216 mm with a weight of 39.1 kg (Tacher et al, 2007).

A Power Conditioning Unit (PCU) was used to adopt the generated voltage to match the vehicle electrical system at 12 and 24 V. The testing of the ETEG was performed on a V8 270 hp gasoline engine of a GM Sierra pickup truck. A precooling heat exchanger was used to asses lowering the inlet temperature of the cooling water. The non effective sides of the ETEG were strictly insulated. The road testing was performed at a vehicles speed of 48.28 km/h, 80.47 km/h and 112.65km/h. The highest generated power and ETEG overall efficiency were obtained at vehicle speed of 112.65 km/h.

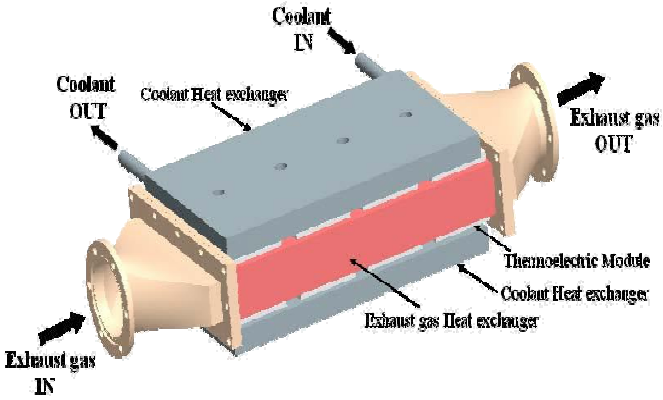

Figure 3.1: Clarkson University ETEG Conceptual Design

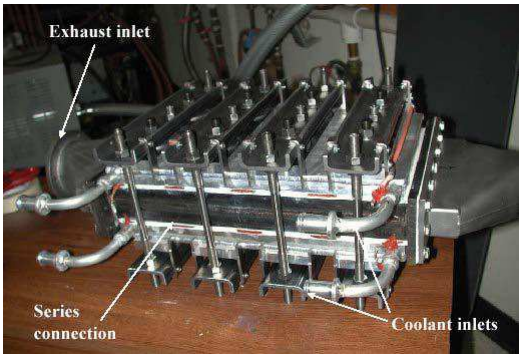

Figure 3.2: Clarkson University ETEG Prototypes

The test results are summarized in the following table:

Table 3.1: Experimental Results from the Clarkson ETEG Road Testing At 112.65 Km/H

Hot-side heat exchanger	
Material	**Carbon Steel**
Thermal Conductivity	50 W/m.K
Working fluid	Exhaust gas
Inlet Temperature	617.3 ºC
Outlet Temperature	484.6 ºC
Cold-Side heat exchanger	
Material	**Aluminum**
Thermal Conductivity	204 W/m.K
Working fluid	Water
Inlet Temperature	86.7 °C
Outlet Temperature	93.9 °C
Test engine	
Maximum power (*Po*)	255.1 W
Engine operating conditions at maximum ETEG power	112.65 km/h Climb up a grade of 7.2%
ETEG overall efficiency at maximum power test (h)	1.66 %
TEM conversion efficiency (h m)	2.8~2.9%

In this case the exhaust pipe between the catalytic converter and the ETEG was insulated with Therm-Tec™ exhaust wrap and aluminum backed with high temperature glass fiber insulation. In flat road testing, the ETEG produced 130.8 W. A maximum power of 255.1 W was measured at a 7.2% graded road test just before the PCU failure which caused the output power to drop precipitously. These results were all measured at a vehicle speed of 112.65 km/h. The targeted 300 W power was never achieved by this ETEG during the road test because of a PCU failure caused the output power to degrade.

CONCEPTUAL DESIGN OF TEG

Discussion of TEG Concepts

The main restrictions governing the design of an exhaust based TEG are to provide sufficient surface area for mounting the modules, achieving heat transfer rate enough to provide the hot and cold surface temperature and maintaining the pressure in the exhaust line without back pressure in the manifold. These three restrictions have been addressed independently in the past literatures. For example, in Clarkson University TEG the first restriction limited the geometry of

the heat exchanger and assembly elements. This failure was explained by the low value of exhaust gas velocity due to large cross sectional area of the hot-side heat exchanger. The dimensions of the hot-side heat exchanger could not be changed to keep sufficient surface area for modules. The TEG introduced by Hi-Z is the first design to address the above mentioned restrictions dependently. Sufficient surface area for mounting the modules was achieved by using a hexagonal cross-section heat exchanger the cross sectional area allowed a minimum pressure drop through the hot-side heat exchanger. Internal fins were applied to enhance the heat transfer from the exhaust gas.

As for the cold-side heat exchanger, all TEG experimentation reported the implementation of aluminum water jackets to provide the cold surface for the thermoelectric modules. Ideally, water is tapped just at the outlet of engine radiator, and passed through the cold-side heat exchanger, then back to the radiator; as shown in figure 4.1

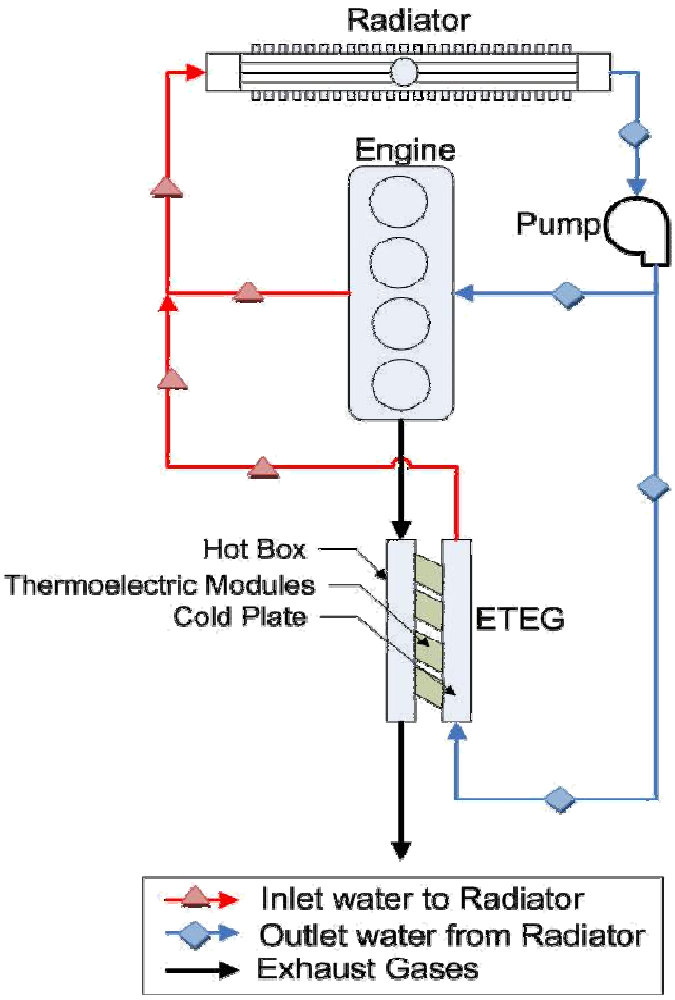

Figure 4.1: Radiator-Engine-TEG Cooling Water /Exhaust Circuit

Another important option for cold-side heat exchanger was investigated by the BSST Thermoelectric Program1, which is funded by the USA Dept. of Energy. This option is to implement a pre-cooling heat exchanger (PCHX) before the radiator and after the TEG, accordingly, separate the water return path of TEG from engine, as shown in figure 4.2. Undoubtedly, the pressure drop in the PCHX and added piping will require the water pump to be replaced. On the other hand, if the PCHX was properly designed, it should have a positive impact on reducing the temperature profile of engine cooling water, hence, enhances the engine thermal efficiency.

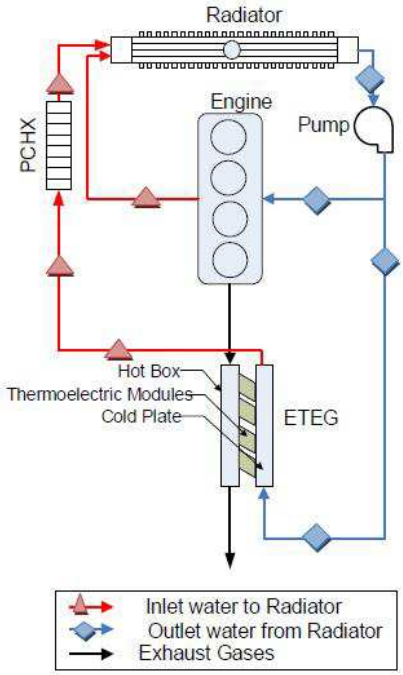

Figure 4.2: The TEG-PCHX Circuit

Iron silicates, silicon germanium and lead/bismuth telluride can be used as thermoelectric materials. The selection of thermoelectric materials is fundamentally based on the operating temperature range. The dilemma of developing high temperature and high efficiency thermoelectric materials is restricting the overall efficiency of TEGs. BiTe modules produced by Hi-Z were reported by GM and Clarkson University in their research. In fact, these modules have proved high performance in power generation more than any other modules available.

Conceptual Design of the Hot-Side Heat Exchanger

The main challenge in conceptualizing the hot-side heat exchanger is to provide sufficient surface area to mount the modules without increasing the flow-cross sectional area of the heat exchanger. To address this challenge, the new concept adopts a circular cross-section heat exchanger with internal longitudinal fins to enhance the heat transfer from exhaust gas. The modules are to be mounted on two surfaces extended longitudinally from the heat exchanger, as illustrated in figure 4.3. The material selected to fabricate the hot-side heat exchanger is UNS C81800 beryllium copper alloy which has a coefficient of thermal conductivity of 218W/m-K. This high thermal conductivity will contribute in increasing the thermal efficiency of the TEG by decreasing the temperature drop between the exhaust gas and TEMs surface. Beryllium copper has good corrosion resistance nearly equal to nickel silver alloys; therefore, this alloy is the most suitable for TEG hot heat exchanger application to resist the effect of sour gases (i.e. SO3 and CO2) of the exhaust gas, and if necessary the inner surface can be electroplated with nickel to enhance the corrosion resistivity of the heat exchanger.

The HZ-20 module dimensions are illustrated in figure 4.4. The nominal generated power for the new TEG concept is 300 Watt. A number of six modules are mounted on each side of the two extended surfaces to achieve this goal.

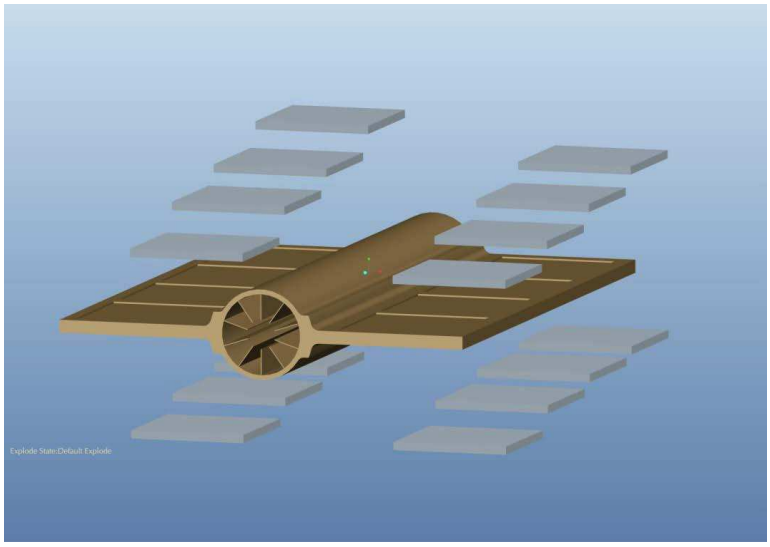

Figure 4.3: Hot-Side Heat Exchanger Concepts

An exploded view showing the assembly of thermoelectric modules on the extended surfaces.

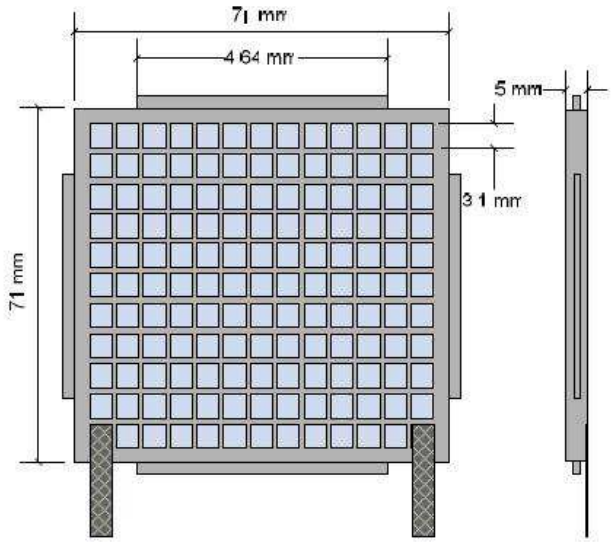

Figure 4.4: Dimensions of a HZ-20 Thermoelectric Module

Conceptual Design of the Cold-Side Heat Exchanger

The cold-side heat exchanger is to be made of aluminum 1100-H20 alloy, which has approximately 99% aluminum and 0.05~0.2% copper among other minor components. This alloy has a coefficient of thermal conductivity equals of 220 W/m- K which is 4.7% higher than pure aluminum. Seven flow paths are created inside the cold-side heat exchanger using 0.8 mm rectangular inserts to increase the overall efficiency of the heat exchanger. The assembly of the cold-side heat exchanger is illustrated in figure 4.5. The presented concept should require less water flow rate to absorb the rejected heat from the thermoelectric modules. Hence, the thermal load added to the radiator is expected to decrease. Another type of cold-side heat exchanger is very interesting to investigate, that is utilizing the vehicle movement to create a turbulent flow around a finned-type heat sink to cool the thermoelectric modules. Such cold-side heat exchanger does not use engine coolant. Therefore, if the finned-type heat sink is optimized for implementation as a TEG cold-side heat

exchanger, there will be no modification required for the engine coolant circuit.

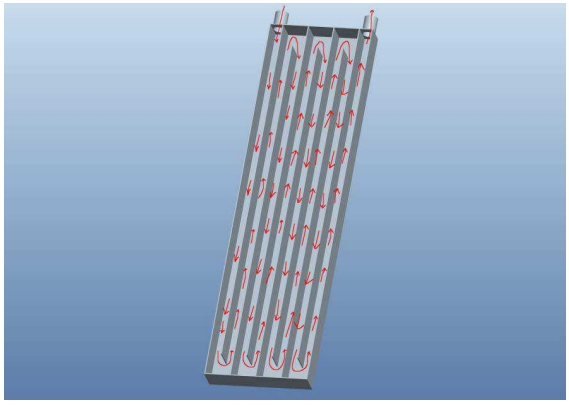

Figure 4.5: Cold-Side Heat Exchanger Showing the Flow Paths

Conceptual Design of the TEG Assembly

In fact, the mounting of thermoelectric modules has a radical effect on the generated power. A compressive loading of 200 psi achieves the highest power generation from a HZ-20 module, if applied on the modules. Such compression would abolish the thermal contact resistance between the module and both surfaces. Additionally, the application of thermal interface material is essential to accentuate the effect of compressive loading. In order to facilitate such procedure, square grooves with 1 mm depth are designed to contain thermoelectric modules on the extended surfaces. Thermal insulation is used to cover all the non-effective surface area of the hot-side heat exchanger to minimize the thermal bypass to ambient air. Figures 4.6 show the full conceptual assembly of the thermoelectric generator.

Increasing the overall efficiency is the main objective in any ETEG design; this increase can be achieved by numerous techniques. The thermal efficiency can be increased by reducing the heat dissipated due to the thermal contact resistance which can be implemented by applying uniform compression to TEMs and using high conductive thermal interface material between the hot and cold sides and the modules. Because the hot box and cold plate are normally electrically conductive, electric insulation should always be applied to the TEMs. Ceramic wafers are ideal to fulfill the thermal interface and electric insulation requirements. A temperature drop of about 10~15°C can now be achieved across these wafers.

For the efficiency of the heat exchanger, it can be controlled by many methods. When the hot box has a relatively large cross sectional area, the exhaust gas velocity is damped when entering the hot box channel. This sudden drop in gas velocity forms a thick thermal boundary layer that causes the overall heat transfer coefficient to be sharply decreased. Internal fins, turbulators and corrugated surfaces are most favourable solutions for eliminating the effect of this boundary layer.

Nevertheless, an important factor should always be considered, the free cross sectional area for the flow. Because if such area is not sufficiently large; the exhaust manifold pressure will be affected causing the engine efficiency to decrease. For the conduction losses through the assembly, the number of assembly elements contacting the hot box directly should be minimized as possible and free surfaces should be strictly insulated.

Thermal insulation is used to prevent the convection from the hot box surface. Nowadays, spray insulation of conductivity as low as 0.03 W/M.K is available and also sustainable for high temperature applications.

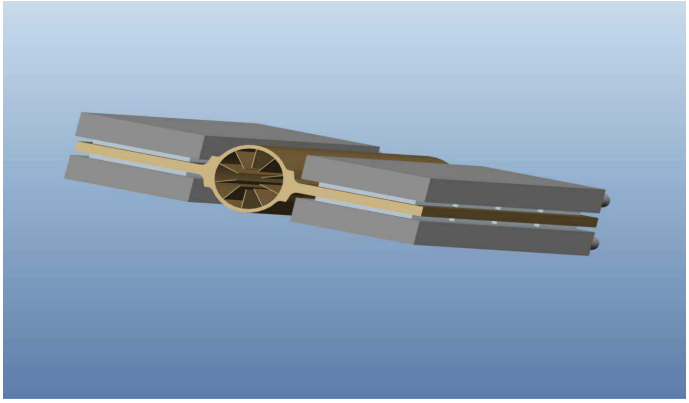

Figure 4.6: TEG Novel Concept

The following tables list out the properties of UNS C81800 Beryllium copper alloy, Aluminum 1100-H20 alloy and the HZ-20 module

Table 4.1 Properties of UNS C81800 Beryllium Copper Alloy

UNSC81800	
Physical properties	
Density	8.9×10^3 kg/m3
Mechanical properties	
Tensile Strength, Ultimate	450 MPa
Tensile Strength, Yield	275 MPa
Elongation at Break	15.0 %
Modulus of Elasticity	110 GPa
Poisson's Ratio	0.330
Shear Modulus	41.0 GPa
Electrical properties	
Electrical Resistivity	0.000359 ohm-mm
Thermal properties	
CTE, linear	18.0 µm/m-°C
Thermal Conductivity	218 W/m-K

Table 4.2: Properties of Aluminum 1100-H20 Alloy

Aluminium 1100 UNS A91100	
Physical properties	
Density	2.71×10^3 kg/m3
Mechanical properties	
Tensile Strength, Ultimate	110 MPa
Tensile Strength, Yield	105 MPa
Elongation at Break	12.0 %
Modulus of Elasticity	75 GPa
Poisson's Ratio	0.330
Shear Modulus	26 GPa
Electrical properties	
Electrical Resistivity	0.0003 ohm-mm
Thermal properties	
CTE, linear	23.6 µm/m-°C
Thermal Conductivity	220 W/m-K

Table 4.3 Properties of HZ-20 module

Properties of the 19 Watt Module, HZ-20	
Physical Properties	
Weight	115 grams
Compressive Yield Stress	70 MPa
Number of active couples	71 couples
Electrical Properties (as a generator)	
Power	19 Watts
Load Voltage	2.38 Volts
Internal Resistance	0.3 Ohm
Current	8 Amps
Open Circuit Voltage	5.0 Volts
Efficiency	4.5 %

CFD ANALYSIS OF TEG

Computational fluid dynamics (CFD) is a branch of fluid mechanics that uses numerical methods and algorithms to solve and analyze problems that involve fluid flows. Computers are used to perform the calculations required to simulate the interaction of liquids and gases with surfaces defined by boundary conditions. With high-speed supercomputers, better solutions can be achieved. Ongoing research, however, yields software that improves the accuracy and speed of complex simulation scenarios such as turbulent flows

CFD Analysis of the Hot-Side Heat Exchanger

A CFD analysis using a turbulence model of the k-ε type was built in ANSYS FLUENT. The boundary conditions and input parameters are detailed in table 5.1. The CFD analysis investigated the effect of flow rate on the pressure gradient inside the heat exchanger as well as the temperature gradient on the extended surfaces. The model has been solved for mass continuity assuming a steady state flow rate entering the heat exchanger and ambient temperature at the outlet side. The pressure gradient is plotted in Figure 5.1. This figure represents the 3-D pressure gradient in the hot-side heat exchanger.

Table 5.1: Boundary Conditions and Input Parameters for the CFD Simulation of Hot Side Heat Exchanger

Heat transfer	Convection and conduction
External heat transfer coefficient	4.5 W/m2.K
Average metal roughness	10 µm
Ambient temperature	293 K
Inlet mass flow	
Flow parameters	Mass flow rate normal to face:
Kg/s	0.047
Thermodynamic parameters	890.3K
Turbulence parameters	Intensity: 2 % Length: 0.0007 m
Boundary layer parameters	Boundary layer type: Turbulent
Outlet static pressure	
Thermodynamic parameters	Static Pressure: 101325 Pa Temperature: 293.2 K
Turbulence parameters	Intensity: 2 % Length: 0.0007 m

Boundary layer parameters	Boundary layer type: Turbulent
Heat transfer	Convection and conduction
External heat transfer coefficient	4.5 W/m2.K
Average metal roughness	10 μm
Ambient temperature	293 K

The temperature gradient along the extended surface for boundary conditions explained in table 5.1 is obtained. Such gradient along the extended surfaces is very important to consider, because it has a direct effect on the generated power. The main advantage of the new conceptual design presented in this research is to achieve low hot-side temperature difference between the first and last module on the extended surface. Such low temperature difference is achieved through depending on conductive other than convective heat transfer through the extended surfaces. A 2-D temperature pattern on the extended surfaces is plotted in Figure 5.2. In addition, the temperature profile along the extended surface centerline (x-x) is plotted in Figure 5.2.

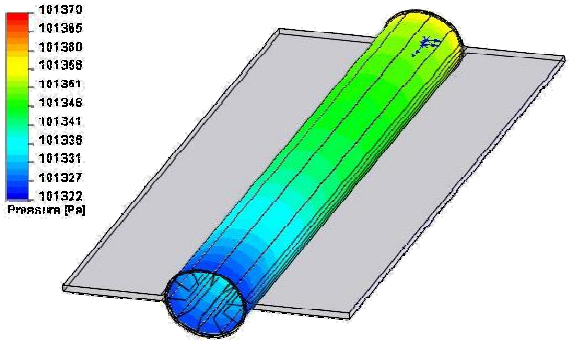

Figure 5.1: Surface Plots for the Pressure Gradient in the Heat Exchanger at 0.047 Kg/S

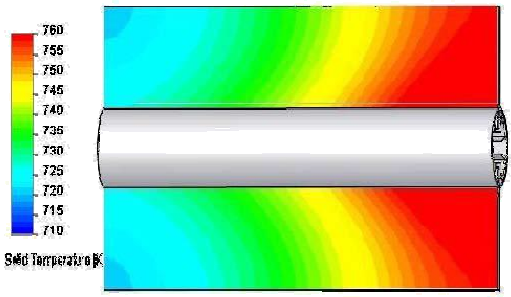

Figure 5.2: Surface Plots for the Temperature Gradient of the Extended Surfaces at 0.047 Kg/S

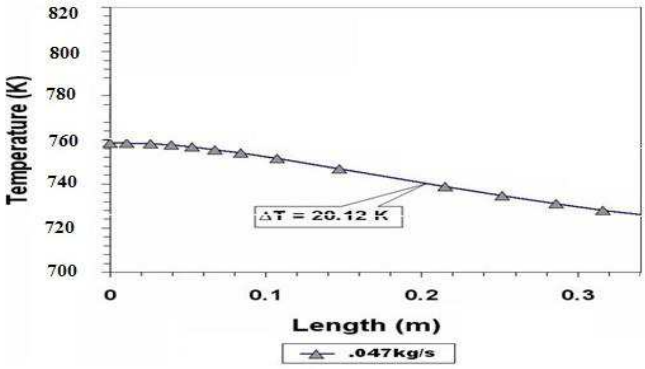

Figure 5.3: Temperature Profile at the Extended Surface Centreline

From Figure 5.3, it is observed that the temperature gradient along the (x-x) axis is an effective gradient, Moreover, the parabolic-shaped temperature contours indicate that the relatively large thickness of the extended surface deviate the heat transfer characteristics in such surface from that of a typical fin. In fact, the temperature gradient across the extended surfaces directly affects the generated power; because such power is a direct function in the temperature difference between the hot and cold sides of the thermoelectric modules.

The main temperature and flow parameters of the hot-side heat exchanger at the examined flow rate values are summarized in table 5.2. The average temperatures in table 5.2 are calculated based on taking the average values of at least 70% of the temperature values on the mesh nodes. This averaging was performed using the postprocessor module of ANSYS FLUENT. The same procedure was followed to get the temperature drop in the exhaust line.

Table 5.2: Summary of the Thermal and Flow Parameters of the Hot-Side Heat Exchanger

Flow rate (kg/s)	0.047
Pressure drop (Pa)	28.68
Average temperature of the extended surface(K)	741.5
Temperature drop on the extended surface (K)	20.12
Temperature drop in exhaust side (K)	12.3
Heat transferred through the hot-side heat exchanger (W)	626

The results shown in Figures 5.1, 5.2 and 5.3, and the parameters discussed in table 5.2 give the preliminary parameters of the thermal performance of the hot-side heat exchanger, and validate the CFD model through the pressure drop results.

CFD Simulation of the Cold-Side Heat Exchanger and TEG Assembly

The assembly described in chapter 4 and illustrated in Figures 4.5 is radically simplified in the present simulation. This simplification is adopted in order to generate results that are more conservative by omitting the positive effect of the assembly elements on the cooling performance of the cold-side heat exchanger. The second reason for adopting this simplification is to reduce the calculations time for the CFD model. Thermoelectric modules are represented as simple thermal resistance with a constant thermal conductivity. The most significant temperature variation is the one parallel to the heat exchanger centreline, for this reason, the assumption that the heat flow through the modules is 1-D is deemed to be valid. The temperature difference between the inlet and outlet of the cold-side heat exchanger should be maintained similar to that between the inlet and outlet of the radiator, if the circuit in Figure 4.1 is to be used.

The axisymmetric of the assembly and flow was used to minimize the computational domain, and variable density meshing was used. The Table 5.3 lists the boundary conditions and input parameters for the TEG assembly analysis. The meshing is a stair-step type mesh. In fact, the flow in both the hot and cold side heat exchangers is characterized by constant cross section geometry and low pressure profile. For this reason, the use of such mesh strategy (i.e. stair-step) along with the standard k-ε turbulence model is expected to deliver accurate and precise results.

2-D temperature patterns of the cold and hot sides of the modules are plotted in Figure 5.4. The temperature gradient on the centerline of the extended surface and the cold-side heat exchanger is plotted in Figure 5.5 for three different exhaust flow rates.

Table 5.3: Boundary Conditions and Input Parameters for the CFD Simulation

Heat transfer	Convection and conduction
External heat transfer coefficient	4.5 W/m2.K
Average metal roughness	10 µm
Ambient temperature	293 K
Inlet mass flow	
Flow parameters	Mass flow rate Flow parameters normal to face 0.165kg/s
Thermodynamic parameters	359.7k
Turbulence parameters	Intensity: 2 % Length: 0.0007 m
Boundary layer parameters	Boundary layer type: Turbulent
Outlet static pressure	
Thermodynamic parameters	Static Pressure: 101325 Pa
Turbulence parameters	Temperature: 293.2 K
Boundary layer parameters	Intensity: 2 % Length: 0.0007 m
Thermal load Heat generation rate (W)	Boundary layer type: Turbulent 626

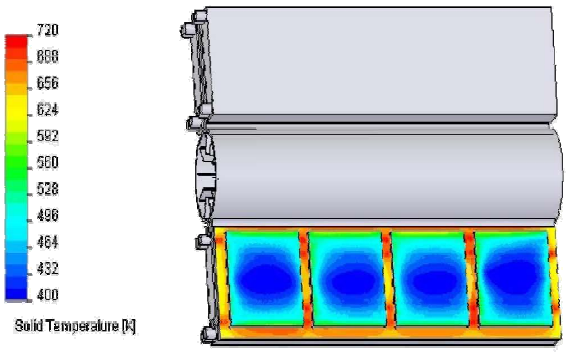

Figure 5.4: Temperature Plots Showing the Cold and Hot Side Temperature Patterns of the Thermoelectric Modules

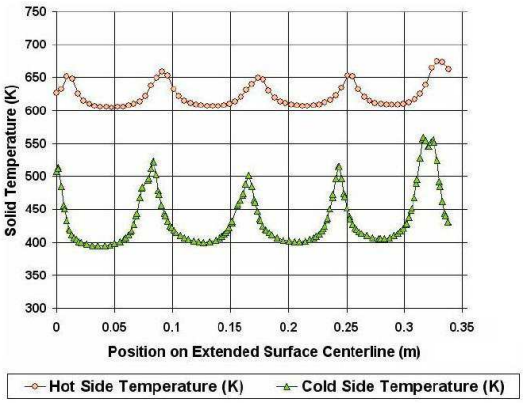

Figure 5.5: Temperature Gradient along the Entreline of Extended Surface

In Figure 5.5, it is obvious that the one dimensional assumption of the heat transfer is valid. This is because the temperature exhibits very large changes along the axial centerline of the extended surface. The sharp ups in the graphs represent the temperature value in between the modules. The temperature distribution on the thermoelectric modules' cold surface takes semi-parabolic shape because of the contact resistance. The temperature difference between the hot and cold sides at the first and last modules represents the "stability" of the TEG thermal performance. When the thermal load is relatively small, the response of the TEG to the cooling effect caused by the cold-side heat exchanger is high, thus, the temperature difference between the cold and hot sides of the first modules is high. For the same reason, the same temperature difference at the first and last modules varies significantly. However, the increase of the thermal load leads to a decrease in the temperature difference between the first module's hot and cold surfaces. On the other hand, the increase in thermal load would enhance the thermal stability of the TEG, in other words, the temperature gradient at the first module will be very similar to that of the last module. As for the pressure and temperature drops in the cold-side heat exchanger, the pressure drop was estimated at 530 Pa at the water flow rate of 0.165 kg/s. The temperature drop ranged from 4 to 5.2 K, which is less than the temperature difference between inlet and outlet sections of the radiator. Table 5.4 shows the thermal operating conditions and corresponding generated power and efficiency.

Table 5.4: Thermal operating conditions and corresponding generated power and efficiency

Surface	HOT SIDE	COLD SIDE
First Module Temperature (K)	610.34	408.55
Last Module Temperature (K)	608.89	409.13
T Average	200.78	
Power per module (W)	18.81	
Input Thermal Energy	574.02	
TEG Power (W)	300.96	
TEG Efficiency	52.43%	

Assessment of the Novel TEG Design

In order to evaluate the novel TEG concept presented in this thesis, the simulation results are compared to the experimental results presented by previous work; the TEGs tested by Clarkson University. The main results for this research were discussed in tables 3.1. The parameters ` of validation and comparison are the mass flow rates, operating temperatures, generated power and the TEG efficiency. The results are compared to the experimental test results of Clarkson University TEG in Table 5.5.

Table 5.5: Comparison of the Performance Characteristics of the Novel TEG and Clarkson Prototype at the Same Thermal Operating Conditions

Case	I		II	
Surface	HOT SIDE	COLD SIDE	HOT SIDE	COLD SIDE
First Module Temperature (K)	610.3	408.5	511.8	387.28
Last Module Temperature (K)	608.8	409.1	495.2	395.7
T Average	200.78		124.53	
Power per module (W)	18.81		8.26	
Input Thermal Energy	570.02		10274.38	
TEG Power (W)	300.96		131.95	
TEG Efficiency	52.43%		1.28%	

The hot and cold side temperatures of the novel TEG concept indicated in column I of table 5.5 have reasonably good agreement with the experimental results from Clarkson TEG, in column II of table 5.5. For the first module, the hot and cold side temperatures obtained from the simulation are 19.23% and 5.49% higher than the experimental result. While for the last module, the hot and cold side temperatures obtained from the simulation are 22.95% and 10.34% higher of the experimental results. The accumulated effects of the increased temperature difference, along with six additional thermoelectric modules have caused the generated power to increase from 131.95 W in Clarkson TEG to 300.96 W for the novel TEG.

CONCLUSIONS AND RECOMMENDATIONS

The significance of thermoelectric waste heat recovery in automotives has been investigated through a literature review. A novel design of an exhaust-based TEG has been developed and presented. The design and simulation for the TEG concept was done. The new concept was assessed through a detailed comparative study with experimental results from Clarkson University. The results of this comparison reveal a large increase in the power of the presented concept over the previous TEG. Such a increase is justified by two main factors; the new geometry of the hot-side heat exchanger and the selection of heat exchanger material.

The TEG geometry was optimized to avoid any backpressure effect on the exhaust manifold. Another important feature in the presented TEG geometry is the utilization of extended surfaces. This feature allowed a large number of thermoelectric modules to be employed on a smaller area compared to the two previous prototypes. The reduction achieved in TEG weight is another positive impact of the geometry, which contributed directly in increasing the TEG power density. The selection of hot-side heat exchanger materials to beryllium-copper alloy radically affected the thermal performance of the TEG as well. Beryllium-copper has a coefficient of thermal conductivity as high as four times of steel. Thus, the conductive thermal resistance decreased significantly, encouraging the temperature pattern along the extended surface to be enhanced at a lower rate of heat transfer.

REFERENCE

1. Bass, J., Elsner, N.B., and Leavitt, A. (1995), Performance of the 1 kW thermoelectric generators for diesel engines. Proc. of the 13th International Conference on Thermo electrics, B. Mathiprakisam, ed., p. 295. AIP Conf. Proc., New York,
2. Fairbanks, J. W. (2005). Thermoelectric Developments for Vehicular Applications, DEER Conference. Detroit,

MI

3. Hi-Z Inc. (1996). Use, Applications, and Testing of Hi-Z Thermoelectric Modules. Hi-Z Inc: Online Catalog available at: http://www.hi-z.com/how-to.htm
4. Kushch, A. S., Bass, J. C., Ghamaty, S. and Elsner, N. B. (2001).
5. Thermoelectric development at Hi-Z technology. Proc. 20th Int. Conf. Thermo electrics, Beijing, China, pp: 422−430.
6. La Grandeur, J., D. Crane and Andreas Eder (2005). Vehicle Fuel Economy Improvement through Thermoelectric Waste Heat Recovery DEER Conference. Chicago, IL.
7. Loffe A.F. (1954) Semiconductors in the Modern Physics, Publishing House of the Academy of Sciences USSR, Moscow-Leningrad.
8. NGKBeryl Co, Beryllium copper's main characteristics, Available at: http://www.ngkberylco.co.uk/B-C.htm